Journal of Autoimmunity 159 (2026) 103533

Contents lists available at ScienceDirect

Journal of Autoimmunity

journal homepage: www.elsevier.com/locate/jautimm

Multiple sclerosis-associated EBNA2 variants influence the response to peginterferon beta-1a therapy

Caterina Veroni [a,2], Fortunata Carbone [b,c,2], Daniela Ricci [d], Stefania Proietti [e], Silvia Romano [f], Maria Chiara Buscarinu [f], Fabiana Rizzo [d], Antonio Marrone [g], Teresa Micillo [h], Francesco Perna [i], Federica Garziano [j], Gisella Guerrera [c], Paola Valentino [k,l], Chiara Meloni [a], Gianmarco Bellucci [f], Antonio Bertolotto [k,m], Luca Battistini [c], Giovanni Ristori [f], Diego Centonze [n,o], Giuseppe Matarese [b,p], Eliana M. Coccia [d], Marco Salvetti [f,o], Martina Severa [d,1], Rosella Mechelli [g,q,1,*]

[a] Department of Neuroscience, Istituto Superiore di Sanità, Rome, Italy
[b] Institute of Endotypes in Oncology, Metabolism and Immunology,National Research Council (IEOMI-CNR), Naples, Italy
[c] Neuroimmunology Unit, IRCCS Fondazione Santa Lucia, Rome, Italy
[d] Department of Infectious Diseases , Istituto Superiore di Sanità, Rome, Italy
[e] Unit of Clinical and Molecular Epidemiology, IRCCS San Raffaele Roma, Rome, Italy
[f] Centre for Experimental Neurological Therapies, Department of Neurosciences, Mental Health and Sensory Organs, Sapienza University, Rome, Italy
[g] IRCCS San Raffaele Roma, Rome, Italy
[h] UOSD Neurologia II, Azienda Ospedaliera Universitaria "Luigi Vanvitelli", Napoli, Italy
[i] Department of Clinical Medicine and Surgery, Federico II University, Naples, Italy
[j] U.O.C. Biochimica Clinica A.O.R.N. Ospedale dei Colli, PresidioMonaldi, Naples, Italy
[k] Neuroscience Institute Cavalieri Ottolenghi (NICO), University Hospital San Luigi Gonzaga of Orbassano, Torino, Italy
[l] Neurology and CRESM (Regional Reference Multiple Sclerosis Centre), University Hospital San Luigi Gonzaga of Orbassano, Turin, Italy
[m] Percorso Sclerosi Multipla, Ospedale Koelliker, Turin, Italy
[n] Department of Systems Medicine, Tor Vergata University, Rome, Italy
[o] Unit of Neurology, IRCCS Neuromed Pozzilli (IS), Italy
[p] Department of Molecular Medicine and Medical Biotechnology,University of Naples Federico II, Naples, Italy
[q] Department of Human Sciences and Quality of Life Promotion, San Raffaele Roma University, Rome, Italy

ARTICLE INFO

Keywords:
Multiple sclerosis
Peg-interferon beta-1a
EBNA2 alleles
IFN-Stimulated gene
Glycolytic capacity
T-lymphocyte phenotyping

ABSTRACT

Background: Strong evidence links Epstein-Barr virus (EBV) infection to Multiple Sclerosis (MS). Peginterferon beta-1a (peg-IFN), currently the most used interferon formulation among first-line treatments in MS, displays immunomodulatory, anti-inflammatory, and antiviral properties and remains also an important therapeutic option in conditions such as pregnancy, lactation and aging patients.
Objectives: In this study we evaluated the ability of peg-IFN to restore a homeostatic EBV-host interaction in MS by regulating antiviral and immunometabolic responses.
Methods: In people with MS (pwMS), peripheral blood mononuclear cells (PBMCs) were analyzed before (T0) and after six months (T6mos) of peg-IFN administration: IFN-stimulated gene (ISG) levels, EBV DNA load, Epstein-Barr nuclear antigen 2 (EBNA2) allele distribution, and T-lymphocyte phenotyping with glycolytic metabolism were assessed.
Results: Peg-IFN increased ISG transcription and glycolysis in $CD4^+$ T lymphocytes, and reduced EBV DNA load without altering EBNA2 allele distribution. Notably, ISG expression increase at T6mos in pwMS infected by the non-risk 1.3B EBNA2 allele, correlating with a better long-term response to peg-IFN after 2-years. Lower T-cell glycolytic capacity at T0 predicted higher peg-IFN responsiveness in pwMS carrying the 1.3B allele, suggesting that EBNA2 variants might be predictive of response to peg-IFN.

* Corresponding author. San Raffaele Roma University, Rome, Italy
E-mail address: rosella.mechelli@uniroma5.it (R. Mechelli).
[1] shared senior authorship.
[2] shared first authorship.

https://doi.org/10.1016/j.jaut.2026.103533
Received 7 November 2025; Received in revised form 9 January 2026; Accepted 23 January 2026
Available online 12 February 2026

Conclusion: Here, we found that infection with MS-associated EBNA2 variants might be involved in the clinical response to peg-IFN therapy. The predictive model developed, which integrates immunological and viral parameters, may help clinicians in a finer selection of first-line therapies tailored to patient profiles, supporting personalized medicine approaches.

1. Introduction

Multiple sclerosis (MS) is a chronic inflammatory disease of the central nervous system (CNS) for whom both genetic predisposition and environmental factors contribute to disease onset and progression [1]. Among environmental triggers, Epstein Barr virus (EBV) infection is recognized as a major risk factor for MS [2] supported by large scale epidemiological studies showing nearly universal EBV seropositivity in adults with MS and elevated anti-EBV antibody titers compared to healthy subjects [3,4]. Recently, a longitudinal study has provided compelling evidence supporting a causal role for EBV in MS, particularly in the earlier stages of the disease [5]. However, the pathogenic mechanisms linking EBV infection to CNS pathology in MS remain unclear [6,7]. Current hypotheses include molecular mimicry, induction of autoantigens [8], immortalization of autoreactive B-cell clones, and impaired immune surveillance of EBV infection in the CNS [9]. Supporting this, EBV-infected B cells have been detected in the post-mortem MS brain [10–12] along with altered antiviral T cell response both in the CNS [13,14] and in the peripheral blood [15] pointing to a defective immune control of a persistent EBV infection [9,16]. In addition, different EBV genetic strains in genetically susceptible individuals might be also involved in MS pathogenesis [17,18]. In particular, the allelic variants of EBV genes encoding proteins participating in the latency phase of infection, including Epstein-Barr nuclear antigen-2 (EBNA2), have been associated with MS [17–19].

Among first-line therapies for MS, interferon-beta (IFN-β) has long been used for its immunomodulatory, anti-inflammatory, and antiviral properties. Pegylated-IFNβ (peg-IFN, Plegridy®, Biogen) is currently the most used IFN-β formulation and was recently associated with higher adherence and lower escalation rates than classical subcutaneous IFN-β-1a toward more effective but more costly drugs [20]. The conjugation of the recombinant IFN-β-1a molecule to a single, linear 20 kDa methoxy poly(ethyleneglycol) molecule at the alpha-amino group of the N-terminal amino acid residue (i.e., pegylation) prolongs, indeed, the half-life of the compound [21,22] and reduces the frequency of dosing, while maintaining safety and efficacy of the active substance [23,24]. Today, as treatment options in the field evolved with newer therapies more effective and better tolerated, IFN-β treatments are however less prescribed as first-line therapy in relapsing remitting (RR) MS. Nonetheless, peg-IFN, together with classic subcutaneous and intramuscular IFN-β formulations, has a place in the field in clinical trial research and remains also an important therapeutic option in clinical practice especially around pregnancy planning and lactation, and may also be considered for aging patients, in which MS activity declines and long-term immunosuppression associated with some alternative therapies is a concern [25].

In two randomized phase I studies evaluating the pharmacodynamic responses of peg-IFN, the regulation of IFN-stimulated genes (ISG) including those encoding 2′,5′-oligoadenylate synthetase (2′,5′- OAS), myxovirus resistance protein 1 (Mx1), ISG15 as well as several chemokines and cytokines such as the anti-inflammatory Interleukin-10 (IL-10), have been analyzed [26].

Besides the well-characterized antiproliferative and immunomodulatory properties of IFN-β [27], this molecule also retains an antiviral activity that likely contributes to MS treatment efficacy and that, however, has been only partially investigated [28].

Because of the solid data supporting an altered EBV-host immune interaction in MS and the likelihood that EBV deregulation is directly involved in MS pathology, in this study we analyzed several EBV-related, immunological, and metabolic parameters aiming at better characterizing the immunomodulatory and antiviral properties of peg-IFN treatment in MS.

Nowadays, a plethora of very effective disease-modifying therapies is available for the treatment of people with MS (pwMS) allowing the personalization of cure and helping clinicians in the choice of the right drug for the right person at the right time. In this context, understanding how peg-IFN treatment impacts on EBV infection and host-pathogen interaction in MS may provide new insights on disease biology and help in identifying the subset of patients in which the timely administration of IFN-β treatment might be more effective.

2. Methods

2.1. Standard protocol approvals, registrations, and patient consents

The study was approved by the local Ethics Committee of Sapienza University (approval ID 1505, February 22, 2017) and was conducted in accordance with Good Clinical Practice guidelines and the ethical principles of the Declaration of Helsinki. Participants were enrolled among patients who had been started on peg-IFN as part of routine clinical practice. After a screening visit to assess eligibility, all participants provided written informed consent prior to inclusion in the study. This was an observational study; therefore, trial registration was not required. No identifiable images or personal information of participants are included in this study.

2.2. Study cohort

Thirty pwMS with a RR disease course defined according to the revised McDonald's criteria [29] were recruited for this study. Enrollment of 27 pwMS was carried out at Centre for Experimental Neurological Therapies (CENTERS), Department of Neurosciences, Mental Health and Sensory Organs (NESMOS) Department, Sapienza University (Rome, Italy). Peripheral blood mononuclear cells (PBMCs) and serum samples from three additional pwMS fulfilling the inclusion criteria for this study have been also provided by CRESM Biobank, AOU San Luigi Gonzaga (Orbassano, Turin, Italy). Blood samples, clinical and demographic parameters were obtained for all subjects immediately before peg-IFN (T0, baseline) after 6 (T6mos) and 12 months (T12mos) of therapy. Clinical information was also collected at 24 months of follow-up. Revision of adverse events and concomitant medications were assessed during each visit. All reasons that led to discontinuation (e.g., occurrence of adverse events, lack of efficacy, safety concern, and patient decision) were recorded and considered during the data analysis phase (Supplementary Table 1). In addition, PBMC samples from 21 healthy donors (HD) were included as a reference group for EBV DNA quantification (17 females and 4 males; median age 34 years, range 21–56).

2.3. Sample collection

Serum samples and PBMCs were obtained as previously described [30]. $CD19^+$ B cells were sorted from PBMCs by magnetic cell separation with the human CD19 Microbeads kit (Miltenyi, Bergisch Gladbach, Germany). $CD8^+$ T cells were isolated from PBMCs by magnetic cell separation with the Dynabeads CD8 Positive isolation kit (Invitrogen, ThermoFisher Scientific). The cell negative fraction was then used for the purification of $CD4^+$ T cells with “Dynabeads Untouched human

CD4 T cells" kit (Invitrogen, ThermoFisher Scientific).

2.4. Anti-EBNA1 IgG quantification

Levels of anti-EBNA1 IgG were assessed in pwMS serum samples collected at T0 using Serion ELISA classic kit (Virion/Serion, Würzburg, Germany), following the manufacturer's instructions.

2.5. RNA isolation and reverse-transcription

Total RNA was isolated by Trizol Reagent (Invitrogen, Thermo Fischer Scientific, Dreieich, Germany). Reverse-transcription was conducted by Vilo reverse transcriptase kit (Invitrogen, ThermoFisher Scientific) [30].

2.6. Quantitative real time PCR analysis

Expression of the genes encoding Mx1, ISG15 and IL-10 was measured by quantitative real time PCR on a ViiA 7 Instrument (Applied Biosystems, ThermoFisher Scientific).

Sample values were normalized by calculating the relative quantity of each mRNA to that of the housekeeping gene TATA box-binding protein (TBP) [31], using formula $2^{-\Delta Ct}$, where ΔCt represents the difference in cycle threshold (Ct) between target mRNA and TBP mRNA.

2.7. Droplet digital PCR for EBV viral load analysis and EBNA2 genotyping

Both viral load quantification and EBNA2 genotype identification have been performed using the droplet digital Bio-Rad QX200 PCR system (Bio-Rad, Hercules, CA, USA). Genomic DNA was extracted from PBMCs (for EBV load analysis in pwMS and HD) and isolated $CD19^+$ B cells (for EBV genotyping) using QIAmp DNA mini kit (Qiagen) following the manufacturer's instructions and then quantified using Nanodrop 2000 (ThermoFisher Scientific).

A mixture of specific fluorescent primers/probes, Droplet PCR Supermix no dUTP and 250 ng of DNA was prepared and emulsified with droplet generator oil using a QX-200 droplet generator (Bio-Rad) according to the manufacturer's instructions. The droplets were subjected to PCR amplification, and then analyzed using a QX200 droplet reader (Bio-Rad). Fluorescence data for each well were analyzed using QuantaSoft software, version 1.7 (Bio-Rad). EBV viral load was assessed for each sample normalizing EBV *Bam*HI-W copy number to the human EIF2C2 internal control. DNA from EBV-positive (B95-8 and NAMALWA) and EBV-negative (BJAB) cell lines has been always included as positive and negative controls, respectively.

2.8. Immuno-phenotypic analyses

Whole blood cells were analyzed with a clinical-grade hemocytometer to determine absolute lymphocyte numbers in each sample. Flow cytometry was carried out by using AQUIOS Tetra-1+ Panel Monoclonal Antibody Reagents consisting of CD45-FITC/CD4-RD1/CD8-ECD/CD3-PC5 and AQUIOS Tetra-2+ Panel Monoclonal Antibody Reagents consisting of CD45-FITC/(CD56+CD16)-RD1/CD19-ECD/CD3-PC5, HLA-DR-PC7 and CD45RO-ECD (Beckman Coulter Life Sciences). Immunophenotypic analysis was performed in $CD45^+$ gated cells with Cytomics FC500 Flow Cytometer (Beckman Coulter Life Sciences) with CXP software (Version 2.0) and Kaluza Analysis Flow Cytometry software (Version 2.1.1).

2.9. Metabolic assays

Purified $CD8^+$ T cells and $CD4^+$ T cells were plated in XFe-96 plates (Seahorse Bioscience) and stimulated for 12 h in the presence of anti-CD3 and anti-CD28-coated (anti-CD3/CD28) Dynabeads (ThermoFischer Scientific). Real-time measurements of the extracellular acidification rate (ECAR) were performed by an XFe96 Analyzer (Seahorse Bioscience, Billerica, MA, USA). ECAR, index of glycolysis, was measured in XF media in basal condition and in response to 10 mM glucose, 5 μM oligomycin and 100 mM of 2-deoxy-d-glucose (2-DG) (Sigma Aldrich, St. Gallen, Switzerland). Indices of glycolytic pathway activation were calculated from ECAR profile: glycolysis (calculated as the difference between ECAR before oligomycin injection and ECAR before glucose injection), and glycolytic capacity (calculated as the difference between ECAR after oligomycin injection and ECAR before glucose injection).

2.10. Statistical analyses

All the data are represented as the mean values with standard error mean (SEM) for continuous variables and as frequencies for categorical variables. Statistical significance of differences in the mean values was analyzed using the paired two-tailed Student's t-test to examine pre- and post-treatment change/variation. When appropriate, non-parametric analyses were performed using the Wilcoxon matched-pairs signed-rank test or the Mann–Whitney test. Where three or more experimental conditions were compared, Two-way Repeated-Measures ANOVA was used as indicated in figure legends. P values ≤ 0.05 were considered statistically significant. In the figures, P values are assigned as follows: * ≤ 0.05; ** ≤ 0.01; *** ≤ 0.001.

To quantify the impact of treatment (after 6 months) on the changes in the EBV copies, IL-10, Mx1 and ISG15 genes, generalized linear mixed (GLM) effects model was used. EBNA2 alleles and biological parameters resulting statistically relevant in the previous analysis were considered as fixed effect components. Age and sex were considered as confounders, and subjects as a random factor to explain the variation at individual level. Results were presented as beta-coefficients, standard error and corresponding 95 % confidence intervals (95 % CI).

Statistical significance was defined using an α-level <0.05: although the presence of many variables, it was decided not to use corrections for multiple comparisons, but to prefer an informative use of statistical significance in order to reveal potential associations to be further tested. All analyses were conducted in SPSS statistical software version 27.0 and GraphPad Prism 8 version 8.4.3.

3. Results

3.1. Characteristics of enrolled patients

In this study we analyzed clinical, virological, and immunological data of 25 pwMS immediately before administration of peg-IFN (T0, baseline) and after 6 months of therapy (T6mos). A detailed flow-chart of the study is included in Fig. 1. Demographic and clinical characteristics are summarized in Supplementary Table 2.

To define the timing of blood withdrawal for this study, the first five enrolled MS patients were sampled at baseline, 1, 7 and 14 days after the first peg-IFN administration of full dose regimen (125 μg). To assess the kinetic of drug activity, we longitudinally measured the gene expression of the ISG Mx1 and ISG15. A major induction of IFN gene signature was observed 1 day after treatment with a progressive reduction of mRNA level over time (Fig. 2A). Thus, for all the assays performed at T6mos, blood samples were collected at this time point post injection.

3.2. Analysis of type I IFN signature in pwMS treated with peg-IFN

To evaluate the biological activity of the drug, in this study we monitored the regulation of ISG expression pattern at T0 and T6mos of peg-IFN treatment (Fig. 2B).

The transcription of two canonical ISG Mx1 and ISG15, as well as of IL-10, an anti-inflammatory/regulatory factor known to be induced in pwMS undergoing IFN-β treatment, was characterized in RNA isolated

Figure 1

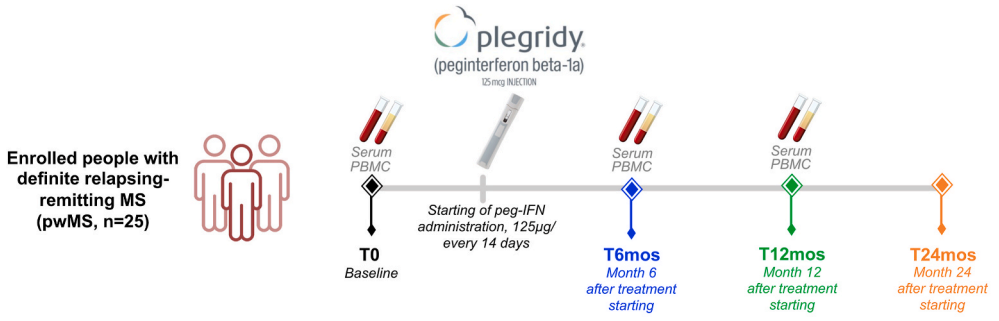

	T0	T6mos	T12mos	T24mos
Neurologic visit, EDSS	◆	◆	◆	◆
Anti-EBNA1 IgG	◆			
Viral load	◆	◆		
EBNA2 genotyping	◆	◆		
IFN response (Mx1/ISG15/IL-10 transcription)	◆	◆	◆	
Immune-phenotyping	◆	◆		
T cell metabolism	◆	◆	◆	

Fig. 1. Flow chart of the study. Scheme of the people with definite relapsing-remitting Multiple Sclerosis (pwMS) enrolled in the study. A schematic representation of the number of study participants, treatment schedule and timeline of sample collection is depicted. Clinical, immunological and viral parameters collected at each time point are reported. All enrolled pwMS (n = 25) were studied before (T0, baseline) and after beta-1a (peg-IFN) treatment (T6mos and T12mos). Clinical information was also collected at 24 months of follow-up.

Figure 2

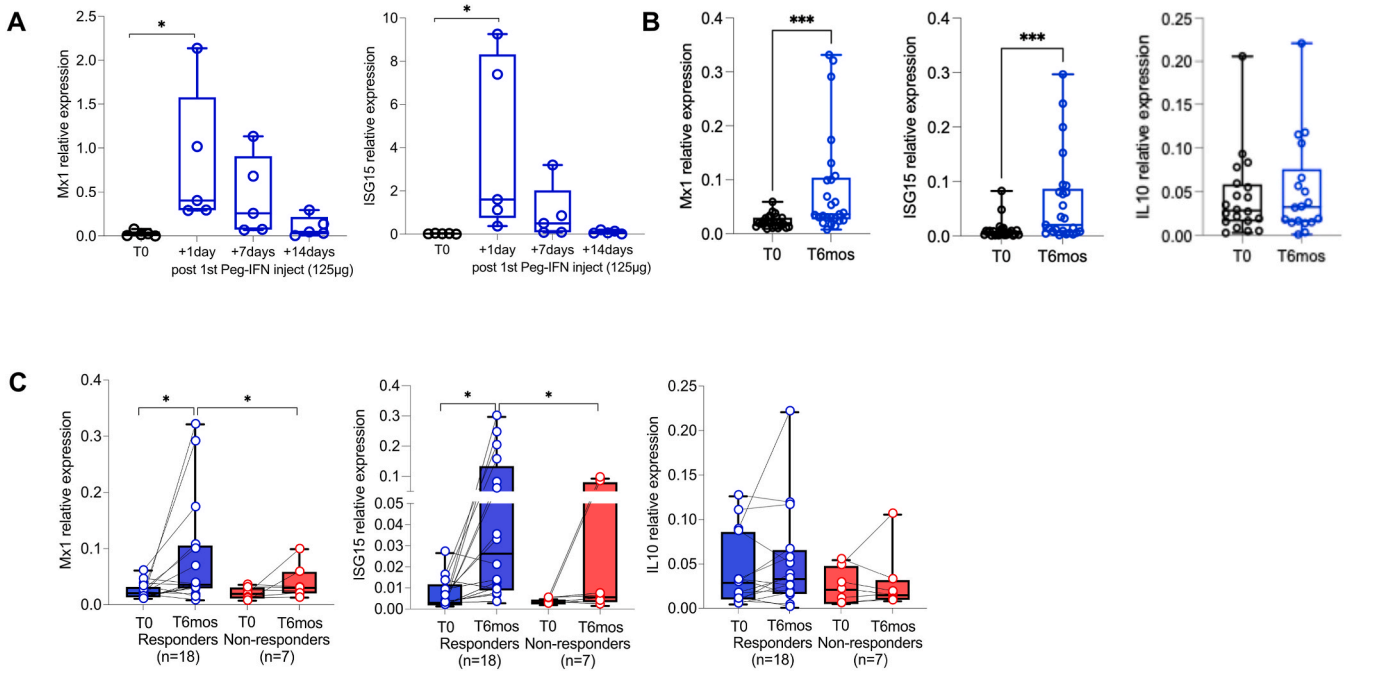

Fig. 2. Quantification of IFN-stimulated gene (ISG) expression in PBMCs of pwMS before and after *in vivo* peg-IFN administration. (**A**) A kinetic study was performed to evaluate by quantitative real time PCR level of expression of two ISG, namely Mx1 and ISG15, in freshly isolated PBMCs derived from the first 5 enrolled pwMS willing to donate their blood before (baseline, T0) and after 1, 7 or 14 days from the first *in vivo* peginterferon beta-1a (peg-IFN) injection of full dose regimen (125 μg). (**B**) Gene expression of Mx1, ISG15 and IL-10 was measured in PBMCs of pwMS (n = 25) at T0 and after 6 months from peg-IFN (T6mos). (**C**) Responders (n = 18) or non-responders (n = 7) to peg-IFN based on inefficacy of therapy at 2-year follow-up were stratified according to their level of quantified ISG expression. Level of mRNA expression was normalized to that of the housekeeping gene TATA-binding protein (TBP) using formula $2^{-\Delta Ct}$. Each dot represents a single analyzed patient at the different studied time points and error bars show median values ± IQR. P-values were calculated by Wilcoxon matched-pairs signed rank test (B) and two-way ANOVA test (C). *P values were assigned as follows: ≤0.05, *** ≤0.001.

from PBMCs of all the enrolled pwMS longitudinally followed at T0 and T6mos (Fig. 2B). *In vivo* peg-IFN administration significantly enhanced the expression of both Mx1 and ISG15 genes at T6mos, while no significant change was observed for IL-10 mRNA level. Gene expression

level did not change significantly when comparing T6mos and T12mos (after 12 months of therapy start), indicating that T6mos reliably reflects the patient's response of the following months at the individual level (Supplementary Fig. 1A).

By using clinical information collected at follow-up visits (see Supplementary Table 1), the patients were operationally classified in responders and non-responders to therapy at 24 months of follow-up: 7 pwMS discontinued peg-IFN due to lack of efficacy, while 18 remained under treatment without disease activity. We found that the responders to therapy showed a higher ISG transcription at T6mos following drug administration (Fig. 2C and Supplementary Fig. 1B), suggesting that monitoring this gene expression levels may be useful for assessing therapy effectiveness over time. In line with this view, in those patients that were followed up to 12 months of therapy, classified into responders or non-responders, ISG expression was induced and remained stable only in the responders' subgroup (Supplementary Fig. 1C).

3.3. Peripheral immunophenotyping and T cell metabolic profiling in pwMS treated with peg-IFN

To further explore the immunological effects of peg-IFN, we performed an extensive immunophenotypic analysis of peripheral blood cells from pwMS before (T0) and after 6 months (T6mos) of treatment. Cytofluorimetric analysis revealed that peg-IFN significantly modulates the number and percentage of circulating immune cell subpopulations (Fig. 3A–F and Supplementary Table 3). Specifically, the absolute number of total leukocytes and lymphocytes resulted reduced. Moreover, within the T cell compartment we observed a reduction at T6mos of the number of T cells with a memory phenotype ($CD3^+CD45RO^+$, $CD4^+CD45RO^+$ and $CD8^+CD45RO^+$) together with a decrease of the percentage of $CD8^+CD45RO^+$ cells (Fig. 3D–F and Supplementary Table 3). On the other hand, we detected an increase in the percentage of T cells with naïve phenotype ($CD3^+CD45RA^+$ and $CD8^+CD45RA^+$) (Supplementary Table 3). The analysis of the other main lymphocyte subsets revealed a significant reduction in the absolute number of $CD16^+CD56^+$ natural killer (NK) cells (Fig. 3C and Supplementary Table 3). No significant differences were observed in the other analyzed immune cell subsets (Supplementary Table 3).

Given the growing recognition that immune cell metabolism regulates immune cell differentiation, fate and function [32], we evaluated the ECAR, indicator of aerobic glycolysis, in $CD4^+$ and $CD8^+$ T cells from pwMS at T0 and T6mos (Fig. 3G–I and Supplementary Fig. 2). Peg-IFN treatment is associated with an increase in glycolytic metabolism in $CD4^+$ T cells (Fig. 3G) as revealed by increased glycolysis (Fig. 3H) and glycolytic capacity (Fig. 3I) at T6mos. Notably, this increase in glycolytic metabolism in $CD4^+$ T cells was also maintained at T12mos compared with T0 (Supplementary Fig. 2D–E). This phenomenon was not observed in $CD8^+$ T cells, which showed no significant change in ECAR over time (Supplementary Fig. 2A–C).

3.4. Effect of peg-IFN treatment on EBV viral load and strain distribution in pwMS

To evaluate a possible antiviral effect of peg-IFN in treated pwMS, we monitored different EBV-related viral parameters. In particular, we first assessed EBV seropositivity of our study cohort at baseline verifying that all serum samples collected at T0 from the enrolled pwMS showed detectable levels of anti-EBNA1 IgG (median value: 4088 U/ml-range: 1730–60012 U/ml).

Next, we evaluated the EBV genome copy numbers in PBMCs from pwMS at T0 and T6mos (Fig. 4A–B). EBV DNA was detected in 60 % of PBMC samples (15/25) at T0 and in 36 % of PBMC samples (9/25) at T6mos. Although not statistically significant, a reduction of both EBV DNA levels and frequency was observed after 6 months of peg-IFN (Fig. 4A–B). When compared to HD, EBV DNA levels measured in PBMCs from pwMS at T0 were significantly higher, whereas after 6 months of treatment (T6mos), both viral load and prevalence appeared more comparable to those observed in HD (Fig. 4A and B).

We then characterized the EBNA2 alleles (i.e., 1.2; 1.3B; 1.3A; B95-8) in DNA samples obtained from $CD19^+$ B cells longitudinally isolated

Figure 3

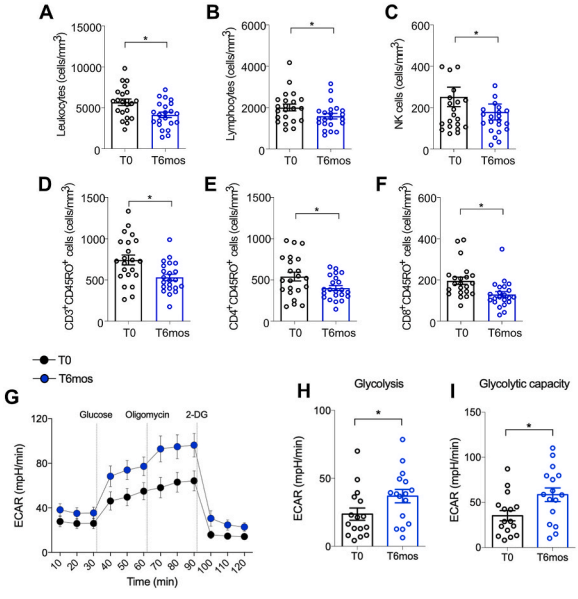

Fig. 3. Regulation of immune-metabolic features in pwMS before and after *in vivo* peg-IFN treatment. (**A-F**) Absolute number per mm^3 of several peripheral blood immune cells in pwMS ($n = 22$) before (T0, baseline) and after 6 months from peginterferon beta-1a (peg-IFN) (T6mos). Comparisons were evaluated using two-tailed paired Student's T-test. P values were assigned as follows: * $\leq$0.05. In particular, leukocytes (**A**), lymphocytes (**B**), NK cells (**C**), $CD3^+CD45RO^+$ (**D**), $CD4^+CD45RO^+$ (**E**) as well as $CD8^+CD45RO^+$ (**F**) T cells are shown and data reported as mean ± S.E.M. (**G-I**) Glycolytic metabolism was evaluated in $CD4^+$ T cells of pwMS (n = 16) at T0 and T6mos. (**G**) The graph represents the kinetic profile of extracellular acidification rate (ECAR) measured in real time under basal conditions and in response to glucose, oligomycin and 2-deoxy-d-glucose (2-DG). Data are shown as mean ± S.E.M. (**H-I**). Indices of glycolytic pathway activation (glycolysis in H and glycolytic capacity in I) calculated from $CD4^+$ T cell ECAR profile. Each dot represents the value from a single subject analyzed and bars show mean ± S.E.M. Statistical analysis was performed by Wilcoxon matched-pairs signed rank test. P values were assigned as follows: * $\leq$0.05.

Figure 4

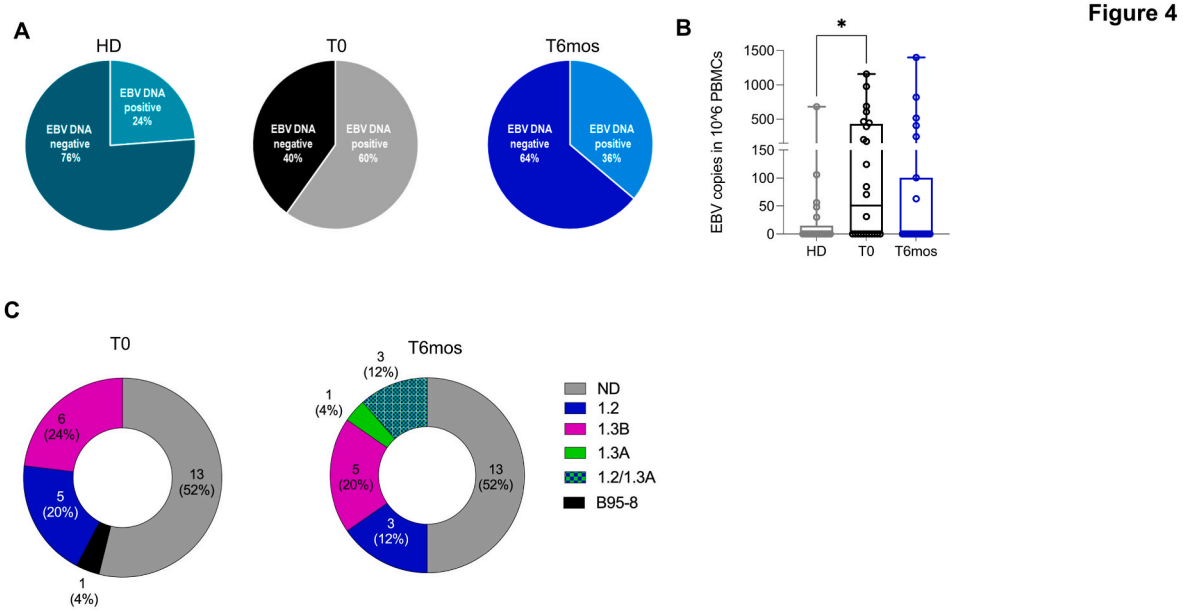

Fig. 4. Viral load and EBV genotype in peripheral blood of pwMS before and after *in vivo* peg-IFN administration. (**A**) Pie charts show the frequency of samples with detectable EBV DNA in HD (n = 21), pwMS (n = 25) before (T0, baseline) and after 6 months of peginterferon beta-1a (peg-IFN) (T6mos). (**B**) Box plots represent EBV copy numbers in PBMCs from HD and pwMS at T0 and T6mos. (**C**) Donut plots show the frequency (number and percentage) of EBNA2 alleles identified in $CD19^{+}$ B cells at T0 and T6mos. Statistical significance was assessed by Mann-Whitney test. P values were assigned as follows: * ≤0.05.

from all the patients (Fig. 4C). The alleles were differently distributed in our study population but remained mostly constant before and after therapy with only little changes. The 1.2 EBNA2 allele was found in 20 % of subjects at T0 (n = 5) and in 12 % at T6mos (n = 3), the 1.3B in 24 % of subjects at T0 (n = 6) and in 20 % at T6mos (n = 5). The B95-8 allele was observed only at T0 in 4 % of subjects (n = 1). The coexistence of two EBNA2 alleles (1.2/1.3A) was observed only at T6mos in 12 % of subjects (n = 3), as well the 1.3A in the 4 % of subjects (n = 1) analyzed. We also found 52 % (n = 13) of undetectable samples (ND) at both T0 and T6mos (Fig. 4C).

3.5. *Multivariate analysis for integration of biological and viral data obtained in pwMS in treatment with peg-IFN*

To integrate the above results and to evaluate the general impact of peg-IFN administration, we applied a multivariate analysis using a

Figure 5

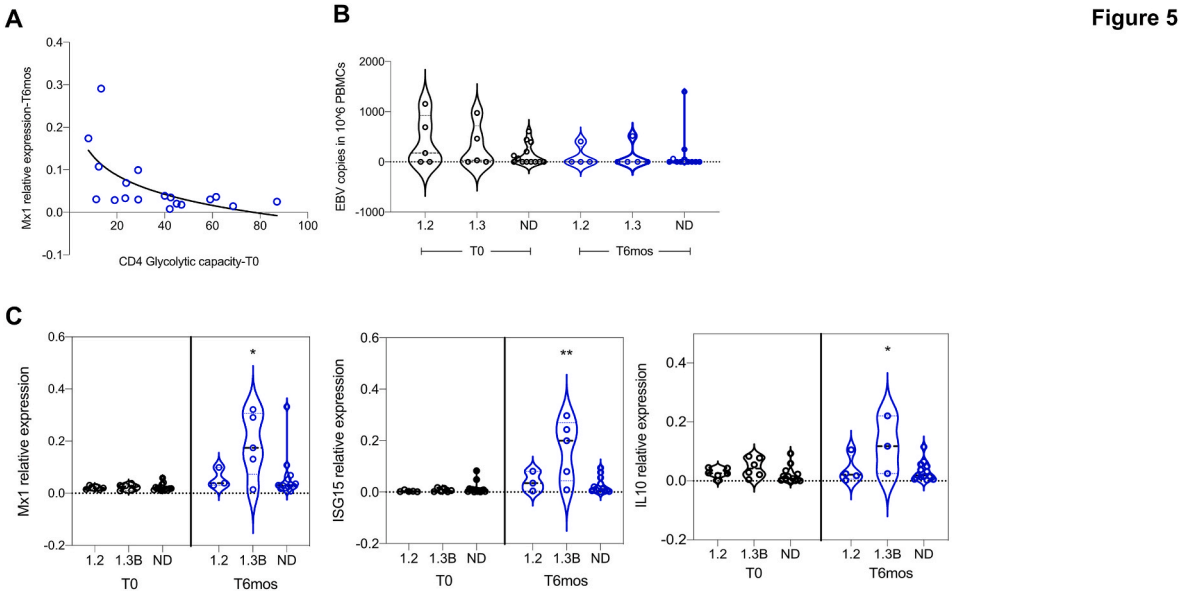

Fig. 5. Impact of EBNA2 alleles on immunological, viral and IFN-related parameters in pwMS before and after peg-IFN treatment. (**A**) The graph shows the non-linear correlation between the level of glycolytic capacity in $CD4^{+}$ T cells detected before peginterferon beta-1a (peg-IFN) treatment (T0, baseline) and the level of Mx1 detected after 6 months of peg-IFN treatment (T6mos). (**B**) Box plots represent the EBV copy numbers in PBMCs of pwMS at T0 and T6mos after classification according to 1.2 or 1.3B EBNA2 alleles ("ND" stands for those samples were EBNA2 alleles were not detected). (**C**) Nested plots show the gene expression level of Mx1, ISG15 and IL-10 grouped by EBNA2 alleles. The mRNA levels were normalized respect to that of housekeeping gene TATA box-binding protein (TBP), using the formula of $2^{-\Delta Ct}$. Each dot represents a single analyzed patient at the different studied time points. P-values were calculated by one-way ANOVA test. P values were assigned as follows: * ≤0.05, ** ≤0.01.

generalized linear mixed effects model.

The results of this analysis did not highlight any contribution of immunophenotyping on the response to peg-IFN therapy. Nevertheless, when we considered the impact of glycolytic capacity of T cells as covariate, we observed that this parameter affected mainly the expression of Mx1. In particular, pwMS with lower levels of $CD4^+$ T cell glycolytic capacity at T0, showed higher levels of Mx1 at T6mos ($\beta = -0.001$; $p = 0.005$; Fig. 5A). Despite the small effect size, likely due to the high inter-individual variability of $CD4^+$ T cell glycolytic capacity, the increase of Mx1 at T6mos, may reflect physiologically meaningful effects.

Furthermore, when we analyzed data on EBV copy numbers according to the detected EBNA2 alleles, we observed a trend of reduction of EBV DNA level at T6mos in both subjects carrying either the 1.2 or the 1.3B allele (Fig. 5B). As expected, the ND samples show the lowest level of EBV DNA in PBMCs irrespective of the treatment.

By further analyzing the impact of EBNA2 genotypes on the other parameters, an interesting piece of data emerged. The presence of the different EBNA2 alleles showed a statistically significant contribution on the level of Mx1, ISG15 and IL-10 expression (Fig. 5C). More specifically, a higher increase of transcript levels was observed at T6mos in pwMS carrying the 1.3B allele compared to the other conditions (1.2 allele and ND respectively, Fig. 5C). This was particularly evident when we considered multiple comparisons: i) the level of Mx1 in 1.3B infected subjects was higher compared to those carrying the 1.2 allele ($\beta = -0.179$, $p = 0.014$) and to the ND group ($\beta = 0.140$; $p = 0.014$); ii) the level of ISG15 was higher in 1.3B infected subjects compared to those carrying the 1.2 allele; iii) IL-10 level in 1.3B infected subject was higher compared to the ND group (Fig. 5C). Interestingly, those individuals carrying the 1.3B allele and showing the highest levels of ISG transcription at T6mos were also among those individuals that better responded to treatment (see Fig. 2C).

Finally, integrating the data obtained by the linear mixed effects model, we constructed the following model predictive of response to peg-IFN therapy considering 1.3B EBNA2 allele at T6mos and the level of $CD4^+$ T cells glycolytic capacity at T0 that emerged as significant contributors, and represented by the following equation:

$$Y = ß_0 + ß_1\ (1.3B) + ß_2\ (CD4 - \text{glycolitic capacity}) + \varepsilon j$$

where "Y" = variable.

"β_0" = intercept
"β_1" = regression coefficient associated with EBNA2 strain
"β_2" = regression coefficient associated with CD4-glycolytic capacity at T0
"εj" = error

This model may help in the definition of the biological conditions that underlie a better peg-IFN response.

4. Discussion

Moving from solid data indicating that an EBV infection is directly involved in MS pathology, in this study we analyzed clinical, virological as well as IFN-related immunological or immunometabolic parameters in a group of pwMS, undergoing peg-IFN treatment, to understand if this drug, through its antiviral effects, may restore a homeostatic EBV-host interaction in MS. Indeed, besides the mechanisms of actions referring to the immunomodulatory and anti-inflammatory activity of IFN-β therapy in MS, this molecule also retains strong antiviral properties in nature, that may target more efficiently the nonheritable (i.e., viral) cause(s) of the disease and that were explored in this study.

Overall, we found that pwMS in treatment with peg-IFN display: i) an induction of the ISG signature, ii) a modulation of the composition of circulating immune cell subsets and a reduction of T cells with memory phenotype, iii) an increase in the glycolytic capacity of $CD4^+$ T cells, and iv) a reducing trend in the level and frequency of EBV DNA, while maintaining a mostly constant distribution of EBNA2 alleles (i.e., 1.2; 1.3B; 1.3A; B95-8). Integrating these multiple analyses, we finally demonstrated that infection with 1.3B EBNA2 allele, in association with some of the other analyzed parameters, may predict the clinical response of pwMS undergoing peg-IFN therapy.

Historically, recombinant IFN-β1 has been the first treatment licensed by FDA for the use in RR MS and its injectable formulations have changed the course of the disease, reducing the relapse rate and the development of new lesions in pwMS [33]. Nowadays, amongst the plethora of MS treatment options available and still increasing, peg-IFN (Plegridy®, Biogen), requiring less frequent dosing as respect to the original molecule, is the IFN-β formulation of choice by clinicians in eligible patients.

To define and score the biological activity of and the response to IFN-β therapy, besides the evaluation of the main clinical and radiological outcomes, surrogate biological markers, such as the transcription of ISG, have been used [34,35]. Many of them have antiviral (i.e., the GTPase Mx1 and the ubiquitin-like protein ISG-15) or anti-inflammatory (i.e., IL-10) activity [34,35]. In line with these evidences, we longitudinally monitored the expression of Mx1, ISG15 and IL-10 in all the enrolled pwMS before (T0) and after 6 months (T6mos) of peg-IFN treatment. *In vivo* administration significantly induced ISG transcription, indicating a good biological activity of the drug in our study cohort. Most interestingly, those patients that at T6mos display the highest level of ISG induction were also those that at 2-year follow up better responded clinically to peg-IFN, while pwMS showing a lower ISG transcription discontinued the therapy for clinical inefficacy. These data may indicate that level of IFN gene signature in the first months after the beginning of peg-IFN treatment could be used as biomarker of long-term response to the drug, also in line with data showed on a subgroup of patients that were followed up to 12 months post therapy and in which no statistically significant difference was found compared to 6 months.

Moreover, in line with the immunomodulatory property of IFN-β, which impact both immune cell frequencies and function [27,36], we performed a detailed immunophenotyping of peripheral blood in pwMS before and after peg-IFN therapy. We found that this pharmacological treatment significantly modifies the composition of circulating immune cell subsets by reducing the absolute number of total leukocytes and lymphocytes. In addition, we observed a decrease in memory T cell subsets. More specifically, after 6 months of therapy, pwMS showed decreased absolute count of $CD3^+CD45RO^+$ as well as $CD4^+CD45RO^+$ and $CD8^+CD45RO^+$ memory T cells together with a reduced frequency of $CD8^+CD45RO^+$ T cells. Conversely, there was a parallel increase in the percentage of naïve T cells, specifically $CD3^+CD45RA^+$ and $CD8^+CD45RA^+$ cells. The observed reduction in memory T cell subsets, together with the relative expansion of naïve T cells, suggests that peg-IFN induces a partial "reset" of the peripheral T cell pool toward a less differentiated phenotype. This shift may reflect both a preferential depletion of antigen-experienced, potentially autoreactive memory T cells and the promotion of a homeostatic balance favouring naïve populations.

It is now well established that, beyond sustaining cell maintenance and growth, metabolic pathways are deeply involved in the regulation of T cell effector functions by shaping their differentiation, activation, and fate [37,38]. Consistent with previous results showing impaired glycolytic capacity in MS T lymphocytes which can be restored by immune therapies such as IFN-β [39], peg-IFN administration specifically increases glycolytic capacity of $CD4^+$ T cells. These data are particularly encouraging as glycolysis is indispensable for induction of regulatory T cells [3,40,41], a cellular subset releasing high levels of the anti-inflammatory IL-10 and involved in immune tolerance by inhibiting the proliferation and effector function of T cells [42,43].

Furthermore, to test the antiviral properties of peg-IFN, we evaluated its impact on EBV infection, the environmental factor with the strongest association to MS [6,7].

In particular, in this study, we have analyzed EBV DNA load before and after treatment with peg-IFN. Even if measuring levels of EBV DNA is not commonly considered as indicator of disease activity, recent evidence suggests that targeting EBV DNA copy number would reduce EBV pathogenesis in MS [44]. Our results indicate that viral load, significantly higher than what found in healthy subjects, tended to decrease and to be less frequently detected in the peripheral blood samples obtained from pwMS 6 months after peg-IFN administration, suggesting that this treatment could alter the virus-host interplay by modulating EBV DNA frequency and levels.

In addition, infection with different EBV genetic strains and their interactions with MS risk genes can also contribute to MS development [45]. Previous studies showed an association between specific EBV variants and MS [17,18], in particular, we found MS-associated alleles within EBNA2 gene, the most variable region of the EBV genome [46]. EBNA2 is a viral transactivator that, in association with human transcription factors, occupies a substantial fraction of risk loci in autoimmune diseases and rewires human gene regulatory programs by rearranging the chromatin landscape [47,48]. The genomic variants we found in the EBNA2 gene significantly influence its function [18]. Notably, our research indicates that the MS-associated 1.2 allele leads to a reduction in CD40 protein levels, a factor previously linked to susceptibility to MS [49]. This finding, along with other supporting evidence, reinforces the importance of EBNA2 and its genetic variants, in modulating the immune response in the infected subjects [50].

Our study showed that peg-IFN therapy had no direct effect on the distribution of analyzed EBNA2 alleles (i.e. 1.2, 1.3B, 1.3A, and B95-8) in pwMS. However, a near significant reduction of EBV viral load emerged when treated pwMS were stratified according to the presence of the different EBNA2 strains. Given the relatively small number of subjects included in this study, these observations need to be validated in a larger cohort.

Interestingly, however, our data also suggest that the EBNA2 1.3B allele, already described as a protective factor for MS [17], could impact on the efficacy of peg-IFN treatment by stimulating higher levels of ISG transcription. Individuals carrying the EBNA2 1.3B allele and displaying the highest ISG level at T6mos were, indeed, also those that better responded clinically to treatment at 2-year follow-up.

By integrating viral and immunological parameters with a multivariate analysis using a generalized linear mixed effects model, we then highlighted that EBNA2 1.3B allele, and the level of $CD4^+$ T cell glycolytic capacity emerged as significant contributors in the efficacy of peg-IFN treatment by impacting on the levels of expression of IFN-inducible genes. Based on this, we developed a predictive model that could allow the definition of the biological conditions that may underlie a better peg-IFN response at the individual level. In this regard, a statistical model that can predict treatment efficacy taking into account the immunological, metabolic and viral background of individual patients could help clinicians in the choice of first-line therapy according to the principle of personalized medicine and also give a contribution and suggestion for other studies willing to assess response to different disease-modifying therapies.

CRediT authorship contribution statement

Caterina Veroni: Writing – review & editing, Writing – original draft, Investigation, Formal analysis, Data curation, Conceptualization. **Fortunata Carbone:** Writing – review & editing, Writing – original draft, Investigation, Formal analysis, Data curation, Conceptualization. **Daniela Ricci:** Methodology, Investigation. **Stefania Proietti:** Software, Formal analysis, Data curation. **Silvia Romano:** Resources, Investigation, Data curation. **Maria Chiara Buscarinu:** Resources, Investigation, Data curation. **Fabiana Rizzo:** Methodology. **Antonio Marrone:** Formal analysis. **Teresa Micillo:** Investigation. **Francesco Perna:** Investigation. **Federica Garziano:** Investigation. **Gisella Guerrera:** Investigation. **Paola Valentino:** Investigation. **Chiara Meloni:** Investigation. **Gianmarco Bellucci:** Investigation. **Antonio Bertolotto:** Investigation. **Luca Battistini:** Funding acquisition. **Giovanni Ristori:** Writing – review & editing. **Diego Centonze:** Funding acquisition. **Giuseppe Matarese:** Funding acquisition. **Eliana M. Coccia:** Writing – review & editing, Funding acquisition. **Marco Salvetti:** Writing – review & editing, Funding acquisition. **Martina Severa:** Writing – review & editing, Writing – original draft, Project administration, Investigation, Formal analysis, Data curation, Conceptualization. **Rosella Mechelli:** Writing – review & editing, Writing – original draft, Investigation, Funding acquisition, Formal analysis, Conceptualization.

Availability of data and material

The raw data collected in course of experiments and used to prepare figures and tables will be shared in an anonymized format only upon request of a qualified investigator to the corresponding author.

Funding

This study was supported by Biogen grant to Centonze D, Matarese G, Battistini L and Salvetti M and partly co-financed by the Italian Ministry of Health (grant GR- 2016-02363749 to Severa M, grant n. GR-2021-12373337 to Carbone F and "Ricerca Corrente" to Mechelli R), by Italian Multiple Sclerosis Foundation (2017/R/18 and 2022/R-Single_064 to Mechelli R, 2022/R-Multi 011 to Veroni C.), Italian Ministry of University and Research (MIUR) (grant n. 2022YMJXYT and grant n. P2022CMK43 to Carbone F), by Horizon-HLTH-2023-DISEASE-3 (Project 101136991; EBV–MS) to Salvetti M and Mechelli R (Project 101137235, BEHIND-MS) to Veroni C, MUR PNRR Extended Partnership (MNESYS no. PE00000006 to Matarese G), Italian Ministry of Health, National Recovery and Resilience Plan (PNRR), Next Generation (EU, M6/C2_CALL 2023, cod to Matarese G) and Finanziamento competitivo di progetti di ricerca (FIN/RIC) 2023 to Mechelli R. The funders had no role in study design, data collection and analysis, decision to publish or preparation of the manuscript. Views and opinions expressed are those of the author(s) only and do not necessarily reflect those of the European Union nor the granting authorities. Neither the European Union nor the granting authorities can be held responsible for them.

Declaration of competing interest

Veroni C., Carbone F, Rizzo F, Proietti S, Ricci D, Buscarinu MC, Romano S, Marrone A, Micillo T, Perna F, Garziano F, Guerrera G, Valentino P, Meloni C, Bellucci G, Severa M, Mechelli R declare no competing interest.

Matarese G reports receiving research grant support from Merck, Biogen, and Novartis and advisory board fees from Merck, Biogen, Novartis, and Roche.

Bertolotto A served on the scientific advisory board of Almirall, Bayer, Biogen, and Genzyme; received speaker honoraria from Biogen, Novartis and Sanofi and grant support from Almiral, Biogen, Associazione San Luigi Gonzaga ONLUS, Fondazione per la Ricerca Biomedica ONLUS, Mylan, Novartis and the Italian Multiple Sclerosis Society.

Salvetti M received research support and consulting fees from Biogen, Merck, Novartis, Roche, Sanofi, Teva.

Salvetti M and Ristori G hold a patent on EBNA2 alleles in multiple sclerosis (IT1417523 EP2981625).

Centonze D is an advisory board member of Almirall, Bayer Schering, Biogen, GW Pharmaceuticals, Merck Serono, Novartis, Roche, Sanofi-Genzyme, and Teva, and received honoraria for speaking or consultation fees from Almirall, Bayer Schering, Biogen, GW Pharmaceuticals, Merck Serono, Novartis, Roche, Sanofi-Genzyme, and Teva. He is also the principal investigator in clinical trials for Bayer Schering, Biogen, Merck Serono, Mitsubishi, Novartis, Roche, Sanofi-Genzyme, and Teva. His preclinical and clinical research was supported by grants from Bayer Schering, Biogen Idec, Celgene, Merck Serono, Novartis, Roche, Sanofi-

Genzyme and Teva.

Battistini L. has served on Scientific Advisory Boards or has given advice to Horizon, Merck, Roche, Teva, Novartis, Bristol Myers Squibb, GSK, and Sanofi-Genzyme; has received speaker honoraria from Horizon, Janssen, Baxter, Merck, Roche, Teva, Biogen, Novartis, Bristol Myers Squibb, GSK, and Sanofi-Genzyme; his preclinical and clinical research was supported by grants from Baxter, Merck, Roche, Teva, Celgene, Novartis and Sanofi-Genzyme; he has also received research support from the Fondazione Italiana Sclerosi Multipla.

The funders had no role in the design of the study, in the collection, analyses, or interpretation of data, in the writing of the manuscript, nor in the decision to publish the results.

Acknowledgments

The authors acknowledge CRESM Biobank, AOU San Luigi Gonzaga, (Orbassano, Turin, Italy) who provided part of the biological samples and associated data used in this study. The authors also thank MS patients who participated in the study by donating their blood.

Appendix A. Supplementary data

Supplementary data to this article can be found online at https://doi.org/10.1016/j.jaut.2026.103533.

Data availability

Data will be made available on request.

References

[1] T. Olsson, L.F. Barcellos, L. Alfredsson, Interactions between genetic, lifestyle and environmental risk factors for multiple sclerosis, Nat. Rev. Neurol. 13 (1) (2017) 25–36.
[2] F. Aloisi, G. Giovannoni, M. Salvetti, Epstein-Barr virus as a cause of multiple sclerosis: opportunities for prevention and therapy, Lancet Neurol. (2023).
[3] S. Abrahamyan, et al., Complete Epstein-Barr virus seropositivity in a large cohort of patients with early multiple sclerosis, J. Neurol. Neurosurg. Psychiatry 91 (7) (2020) 681–686.
[4] K.L. Munger, et al., Anti-Epstein-Barr virus antibodies as serological markers of multiple sclerosis: a prospective study among United States military personnel, Mult. Scler. 17 (10) (2011) 1185–1193.
[5] K. Bjornevik, et al., Longitudinal analysis reveals high prevalence of Epstein-Barr virus associated with multiple sclerosis, Science 375 (6578) (2022) 296–301.
[6] F. Aloisi, A.H. Cross, MINI-review of Epstein-Barr virus involvement in multiple sclerosis etiology and pathogenesis, J. Neuroimmunol. 371 (2022) 577935.
[7] F. Wahbeh, J.J. Sabatino, Epstein-Barr virus in multiple sclerosis: past, present, and future, Neurol Neuroimmunol Neuroinflamm 12 (6) (2025) e200460.
[8] N. Sattarnezhad, et al., Antibody reactivity against EBNA1 and GlialCAM differentiates multiple sclerosis patients from healthy controls, Proc. Natl. Acad. Sci. U. S. A. 122 (11) (2025) e2424986122.
[9] C. Veroni, F. Aloisi, The CD8 T cell-epstein-barr Virus-B cell trialogue: a central issue in multiple sclerosis pathogenesis, Front. Immunol. 12 (2021) 665718.
[10] B. Serafini, et al., Dysregulated Epstein-Barr virus infection in the multiple sclerosis brain, J. Exp. Med. 204 (12) (2007) 2899–2912.
[11] A. Hassani, et al., Epstein-Barr virus is present in the brain of most cases of multiple sclerosis and may engage more than just B cells, PLoS One 13 (2) (2018) e0192109.
[12] N. Orr, L. Steinman, Epstein-Barr virus and the immune microenvironment in multiple sclerosis: insights from high-dimensional brain tissue imaging, Proc. Natl. Acad. Sci. U. S. A. 122 (11) (2025) e2425670122.
[13] B. Serafini, et al., Epstein-Barr virus-specific CD8 T cells selectively infiltrate the brain in multiple sclerosis and interact locally with virus-infected cells: clue for a virus-driven immunopathological mechanism, J. Virol. 93 (24) (2019).
[14] G.P. van Nierop, et al., Intrathecal CD8 T-cells of multiple sclerosis patients recognize lytic Epstein-Barr virus proteins, Mult. Scler. 22 (3) (2016) 279–291.
[15] D.F. Angelini, et al., Increased CD8+ T cell response to Epstein-Barr virus lytic antigens in the active phase of multiple sclerosis, PLoS Pathog. 9 (4) (2013) e1003220.
[16] C. Munz, Altered EBV specific immune control in multiple sclerosis, J. Neuroimmunol. 390 (2024) 578343.
[17] R. Mechelli, et al., Epstein-Barr virus genetic variants are associated with multiple sclerosis, Neurology 84 (13) (2015) 1362–1368.
[18] R. Mechelli, et al., A disease-specific convergence of host and Epstein-Barr virus genetics in multiple sclerosis, Proc. Natl. Acad. Sci. U. S. A. 122 (14) (2025) e2418783122.
[19] D. Varvatsi, et al., Association of Epstein-Barr virus latently expressed genes with multiple sclerosis, Mult Scler Relat Disord 52 (2021) 103008.
[20] M. Moccia, et al., Utilization of ocrelizumab within different treatment strategies for multiple sclerosis: a 5-Year population-based Study, Neurol. Int. 16 (2) (2024) 394–405.
[21] P.A. Calabresi, et al., Pegylated interferon beta-1a for relapsing-remitting multiple sclerosis (ADVANCE): a randomised, phase 3, double-blind study, Lancet Neurol. 13 (7) (2014) 657–665.
[22] B.C. Kieseier, et al., Peginterferon beta-1a in multiple sclerosis: 2-year results from ADVANCE, Mult. Scler. 21 (8) (2015) 1025–1035.
[23] V. Gaberc-Porekar, et al., Obstacles and pitfalls in the PEGylation of therapeutic proteins, Curr. Opin. Drug Discov. Dev 11 (2) (2008) 242–250.
[24] B.C. Kieseier, P.A. Calabresi, PEGylation of interferon-beta-1a: a promising strategy in multiple sclerosis, CNS Drugs 26 (3) (2012) 205–214.
[25] C.H. Goldschmidt, L.H. Hua, Re-Evaluating the use of IFN-beta and relapsing multiple sclerosis: safety, efficacy and place in therapy, Degener. Neurol. Neuromuscul. Dis. 10 (2020) 29–38.
[26] X. Hu, et al., A novel PEGylated interferon beta-1a for multiple sclerosis: safety, pharmacology, and biology, J. Clin. Pharmacol. 52 (6) (2012) 798–808.
[27] M. Severa, et al., IFN-beta and multiple sclerosis: cross-talking of immune cells and integration of immunoregulatory networks, Cytokine Growth Factor Rev. 26 (2) (2015) 229–239.
[28] V. Annibali, et al., IFN-beta and multiple sclerosis: from etiology to therapy and back, Cytokine Growth Factor Rev. 26 (2) (2015) 221–228.
[29] A.J. Thompson, et al., Diagnosis of multiple sclerosis: 2017 revisions of the McDonald criteria, Lancet Neurol. 17 (2) (2018) 162–173.
[30] M. Severa, et al., A cell type-specific transcriptomic approach to map B cell and monocyte type I interferon-linked pathogenic signatures in Multiple Sclerosis, J. Autoimmun. 101 (2019) 1–16.
[31] E. Giacomini, et al., Thymosin-alpha1 expands deficient IL-10-producing regulatory B cell subsets in relapsing-remitting multiple sclerosis patients, Mult. Scler. 24 (2) (2018) 127–139.
[32] M.D. Buck, et al., Metabolic instruction of immunity, Cell 169 (4) (2017) 570–586.
[33] No-Authors-Listed], Randomised double-blind placebo-controlled study of interferon beta-1a in relapsing/remitting multiple sclerosis. PRISMS (Prevention of Relapses and Disability by Interferon beta-1a subcutaneously in Multiple Sclerosis) Study Group, Lancet 352 (9139) (1998) 1498–1504.
[34] S. Malhotra, et al., Search for specific biomarkers of IFNbeta bioactivity in patients with multiple sclerosis, PLoS One 6 (8) (2011) e23634.
[35] M. Comabella, K. Vandenbroeck, Pharmacogenomics and multiple sclerosis: moving toward individualized medicine, Curr. Neurol. Neurosci. Rep. 11 (5) (2011) 484–491.
[36] F. Rizzo, et al., Interferon-beta therapy specifically reduces pathogenic memory B cells in multiple sclerosis patients by inducing a FAS-mediated apoptosis, Immunol. Cell Biol. 94 (9) (2016) 886–894.
[37] H. Chi, Immunometabolism at the intersection of metabolic signaling, cell fate, and systems immunology, Cell. Mol. Immunol. 19 (3) (2022) 299–302.
[38] D. Wilfahrt, G.M. Delgoffe, Metabolic waypoints during T cell differentiation, Nat. Immunol. 25 (2) (2024) 206–217.
[39] C. La Rocca, et al., Immunometabolic profiling of T cells from patients with relapsing-remitting multiple sclerosis reveals an impairment in glycolysis and mitochondrial respiration, Metabolism 77 (2017) 39–46.
[40] V. De Rosa, et al., Glycolysis controls the induction of human regulatory T cells by modulating the expression of FOXP3 exon 2 splicing variants, Nat. Immunol. 16 (11) (2015) 1174–1184.
[41] V.A. Gerriets, J.C. Rathmell, Metabolic pathways in T cell fate and function, Trends Immunol. 33 (4) (2012) 168–173.
[42] D.A. Vignali, L.W. Collison, C.J. Workman, How regulatory T cells work, Nat. Rev. Immunol. 8 (7) (2008) 523–532.
[43] S. Dikiy, A.Y. Rudensky, Principles of regulatory T cell function, Immunity 56 (2) (2023) 240–255.
[44] A. Afrasiabi, et al., The interaction of Multiple Sclerosis risk loci with Epstein-Barr virus phenotypes implicates the virus in pathogenesis, Sci. Rep. 10 (1) (2020) 193.
[45] R. Mechelli, et al., Reworking GWAS data to understand the role of nongenetic factors in MS etiopathogenesis, Genes 11 (1) (2020).
[46] D.J. McGeoch, D. Gatherer, Lineage structures in the genome sequences of three Epstein-Barr virus strains, Virology 359 (1) (2007) 1–5.
[47] V.A. Ricigliano, et al., EBNA2 binds to genomic intervals associated with multiple sclerosis and overlaps with vitamin D receptor occupancy, PLoS One 10 (4) (2015) e0119605.
[48] J.B. Harley, et al., Transcription factors operate across disease loci, with EBNA2 implicated in autoimmunity, Nat. Genet. 50 (5) (2018) 699–707.
[49] I. Smets, et al., Multiple sclerosis risk variants alter expression of co-stimulatory genes in B cells, Brain 141 (3) (2018) 786–796.
[50] S. Delecluse, et al., Epstein-Barr virus induces aberrant B cell migration and diapedesis via FAK-dependent chemotaxis pathways, Nat. Commun. 16 (1) (2025) 4581.